Soil & Tillage Research 196 (2020) 104448

Contents lists available at ScienceDirect

Soil & Tillage Research

journal homepage: www.elsevier.com/locate/still

Molecular dynamics of organic matter in a tilled soil under short term wheat cultivation

Marios Drosos[a,b,*], Giovanni Vinci[b], Riccardo Spaccini[b], Alessandro Piccolo[b,**]

[a] Institute of Resource, Ecosystem and Environment of Agriculture (IREEA), Nanjing Agricultural University, 1 Weigang Road, 210095, Nanjing, China
[b] Centro Interdipartimentale di Ricerca sulla Risonanza Magnetica Nucleare per l'Ambiente, l'Agroalimentare ed i Nuovi Materiali (CERMANU), Università di Napoli Federico II, via Università 100, 80055, Portici, Italy

ARTICLE INFO

Keywords:
SOM
Humeomics
Wheat

ABSTRACT

Soil organic matter (SOM) or humus is essential for the agricultural and environmental functionality of soils. Humus comprises small-size heterogeneous organic molecules arranged in complex meta-stable suprastructures, whose composition can be greatly affected by land management. Here, we report the molecular dynamics of the fractions extracted from an agricultural soil cropped with wheat after one and three years of tillage. The total molecular components, named Humeome, of soil under wheat found in both hydrosoluble and organosoluble fractions isolated by the Humeomic procedure, as determined by GC–MS and high-resolution Orbitrap LC–MS, were compared to the Humeome characterized in the same soil when cropped with maize. While the three-years tillage did not vary the total soil organic carbon under both wheat and maize, the carbon recovered for the sum of Humeomic fractions isolated from soil was significantly larger for maize than for wheat, thus suggesting a general destabilization of SOM under wheat cropping. Moreover, the soil Humeome under wheat resulted more hydrophilic than under maize. While fatty acids and carbohydrates were periodically replenished by crop residues, nitrogen-containing molecules, such as amides and heterocyclic nitrogen, and iron-bound molecular systems were the SOM components mostly reduced under wheat. The losses of these compound classes from the soil Humeome was possibly attributed to the exudation differences between wheat and maize cropping. These results reveal that the molecular dynamics and stability of SOM molecular components can be controlled by crops even in a short term.

1. Introduction

World soils contain the greatest reservoir of organic carbon (OC) in the biosphere (Batjes, 2014), and innovative measures to reduce OC losses from soils are required to limit global changes (Minasny et al., 2017; Piccolo et al., 2018). Nevertheless, agriculture intensification to produce food for an increased population will inevitably put soil at risk of SOM degradation and fertility losses (Lal, 2009), thus menacing human sustainability on the planet. Due to the still large uncertainty in strategies to sequester OC in soil (Baveye et al., 2018), there is an urgent need to enlarge knowledge on SOM dynamics, in order to control soil OC and prevent degradation of soil fertility.

Humus represents the metabolic substrate for soil microbial activity that, in turn, continues to transform the bioavailable humic pools until a new equilibrium is established between microbial communities, humic matter and plant species (Basler et al., 2015). While the concept of ecological succession was introduced as a theory (Putnam, 1994), few reports were so far published on the molecular changes of humus due to plant species, even though plant rhizodeposition is reckoned to play an important role in OC turnover in soil (Hütsch et al., 2002; Wang et al., 2006). Larger microbial and CO_2-C exudates were reported in wheat than in maize (Marx et al., 2007), while wheat residues were found to rapidly and persistently stimulate a microbial degradation of fresh organic matter (Bernard et al., 2007), thereby enhancing mineralization of rhizospheric SOM (Schenck zu Schweinsberg-Mickan et al., 2012). Though the long-term wheat cultivation was confirmed to accelerate SOM transformation, heterocyclic nitrogen (HN) was identified by Fourier-transform infrared photoacoustic spectroscopy (FTIR-PAS) as the most stable compound class (Du et al., 2014). Moreover, wheat straw decomposition in soils was recently found to influence SOM

* Corresponding author at: Institute of Resource, Ecosystem and Environment of Agriculture (IREEA), Nanjing Agricultural University, 1 Weigang Road, 210095, Nanjing, China.
** Corresponding author at: Centro Interdipartimentale di Ricerca sulla Risonanza Magnetica Nucleare per l'Ambiente, l'Agroalimentare ed i Nuovi Materiali (CERMANU), Università di Napoli Federico II, via Università 100, 80055, Portici, Italy.
E-mail addresses: drosos.marios@gmail.com (M. Drosos), alessandro.piccolo@unina.it, drososmarios@njau.edu.cn (A. Piccolo).

https://doi.org/10.1016/j.still.2019.104448
Received 3 January 2019; Received in revised form 3 October 2019; Accepted 8 October 2019
Available online 06 November 2019

molecular composition by enriching with alkyl C particulate and mineral-associated OM (Chen et al., 2018).

The acknowledgment of the supramolecular nature of soil humus (Piccolo, 2002, 2016) allowed to develop a novel SOM fractionation sequence, called Humeomics, that not only enabled separation of OC from soil up to 3.6 times more efficiently than by traditional extraction methods (Drosos and Piccolo, 2018), but also enhanced identification of single humic molecules by advanced analytical techniques, such as high resolution ESI-Orbitrap and GC–MS (Drosos et al., 2017; Drosos and Piccolo, 2018; Drosos et al., 2018a). Humeomics progressively isolates molecules which are unbound to the humic suprastructure or released from hydrolyzed esters and ethers (Nebbioso and Piccolo, 2011; Drosos et al., 2018b), or from organomineral associations (Drosos et al., 2017; Drosos and Piccolo, 2018). This methodology was previously used to describe the soil Humeome (defined as the complete set of humic molecules in soil organic matter) present in a sandy loam soil under maize cropping after one and three years of tillage (Drosos and Piccolo, 2018), whereas here we applied Humeomics on the same soil but under wheat cropping. The aim of this work was thus to verify whether wheat cropping may have resulted in a different molecular composition from that determined under maize for the same tillage time lapses.

2. Materials and methods

2.1. Soil

The Typic Ustifluvent soil (Eutric Fluvisol by FAO-Unesco) was sampled from the experimental station of the University of Torino (44°53′N, 7°41′E, 232 m a.s.l) after one (2006) and three (2008) years of continuous conventional tillage. The soil had a sandy loam textural class (63% sand, 30% silt and 7% clay), pH 8, and a content of 75 ppm K_2O and 35 ppm P_2O_5. The soil had been fertilized with urea at the rate of 130 kg ha^{-1} of N and tilled by moldboard plowing 35 cm deep, followed by surface harrowing. Wheat (*Triticum aestivum* L., cv. Blasco) was cropped in 10 m^2 field plots in a completely randomized design of 3 plot replicates and 100 kg ha^{-1} of P_2O_5, and 200 kg ha^{-1} of K_2O per plot (Grignani et al., 2012).

2.2. Alkaline extractable SOM (eSOM)

The eSOM fraction was extracted in triplicates from100 g of surface soil (0–30 cm depth) using 0.9 L of an alkaline solution (0.5 M NaOH + 0.1 M $Na_4P_2O_7$). After overnight shaking, eSOM was separated from soil by centrifugation (15 min, 4500 rpm), filtered through a Whatman 41 filter, and adjusted to pH 7 with 37% HCl. The extract was dialyzed against distilled water using Amicon C membrane (1000 Da cutoff) to remove residual salts and freeze-dried. The eSOM extract amounted to 1086 (± 20) mg for the 1st year, and 1019 (± 30) mg for the 3rd year (Table 1).

2.3. Humeomics sequential fractionation

Triplicates of 100 g of surface soil (0–30 cm depth) were placed in 300 mL of 0.1 M HCl and shaken overnight. Each sample was centrifuged (15 min, 4500 rpm), and air-dried. The Humeomics fractionation was applied as previously described (Drosos and Piccolo, 2018), in order to obtain an unbound fraction (ORG1), weakly bound ester fractions (ORG2 and AQU2), strongly bound ester fractions (ORG3 and AQU3), strongly bound ether fraction (AQU4), and residual OM from final soil (RESOM).

In particular, ORG1 was extracted under stirring for 24 h at room temperature from 100 g of washed soil suspended in 300 mL of a 2:1 v/v dichloromethane (DCM) and methanol (MeOH) solution. The supernatant was separated by centrifugation (15 min, 7500 rpm) and filtration. The remaining soil residue was air-dried.

The residue from ORG1 was placed in a Teflon tube added with 12% BF_3-MeOH (1 g of soil/1 mL of solution) and kept under N_2 atmosphere overnight at 85 °C. This transesterification was repeated twice, and the supernatants were centrifuged (15 min, 7000 rpm), and combined. The resulting solution was added with water to quench the residual BF_3, rotoevaporated to remove MeOH, and extracted three times with a total of 150 mL of chloroform. The organic phase was separated (ORG2), dried with anhydrous Na_2SO_4, filtered on a Whatman 41 filter, and rotoevaporated. The aqueous phase (AQU2) was rotoevaporated to remove residual MeOH and chloroform traces, and dialyzed against distilled water using Amicon C membranes (1000 Da cutoff) until Cl-free, and freeze-dried. The remaining solid residue was air-dried.

The residue from ORG2 was suspended (w/v, 1 g/1 mL) in a 1 M KOH solution in MeOH, and refluxed for 2 h at 70 °C under N_2 atmosphere. After cooling, the reaction mixture was centrifuged (10 min, 4500 rpm) and the supernatant recovered. The residue was washed with 50 mL of MeOH and centrifuged. The supernatants were combined, the pH adjusted to 2.0 with 37% HCl, and then liquid-liquid extracted three times with a total of 150 mL (50:50, v/v) of DCM/water mixture. The organosoluble (ORG3) and hydrosoluble (AQU3) extracts were purified as for ORG2 and AQU2. The remaining solid residue was air-dried.

A suspension of 1 mL of 47% HI aqueous solution per g of soil residue from ORG3 was stirred for 48 h at 75 °C under N_2 atmosphere. After cooling, 100 mL of distilled water were added, stirred and filtered. The solution was neutralized by saturated $NaHCO_3$ solution, freeze-dried, and dialyzed (1000 Da cut-off membranes) first against a saturated $Na_2S_2O_3$ solution to neutralize I_2, and then, against distilled water to remove residual $Na_2S_2O_3$. The resulting suspension (AQU4) was freeze-dried.

The residual soil was washed extensively with water and subjected to extraction by alkaline solution (as for eSOM) of humic molecules tightly-bound to the soil inorganic matrix, representing a residual organic matter (RESOM).

2.4. eSOM and Humeomic fractions characterization

The organosoluble extracts (ORG1-3) were analysed by GC–MS, while the molecular composition of hydrosoluble (AQU2-4), RESOM and eSOM was characterized by high resolution ESI-Orbitrap-MS. The C, H, N content was determined by Elemental Analysis (Table 1), while the iron content in soil was analysed by Atomic Adsorption Spectrophotometry.

2.4.1. GC–MS

Organosoluble fractions (ORG1-3) were methylated before GC–MS analysis using acetyl chloride/methanol, and then silylated using *N,N*-bis [trimethylsilyl] trifluoracetamide/1% trimethylchlorosilane. Quantitative data were obtained adding nonadecanoic acid as internal standard, followed by an external calibration curve of specific standards for the different classes of compounds. Methylated and silylated compounds were converted to nominal masses by adding the H^+ mass and removing methyl and silyl groups, when needed. Chemical structures were obtained by NIST library. The peaks selected for identification were the ones exceeding the cut-off limit of 0.05% of the overall chromatographic area. Identified peaks were then recalculated to match an overall relative percentage of 100.

2.4.2. High resolution ESI-Orbitrap-MS

Two milligrams of eSOM, hydrosoluble fractions (AQU2, AQU3 and AQU4) and RESOM were weighed, spiked with 20 µg each of the two internal standards 16-d3-hexadecanoic acid and ring ^{13}C labelled hydroxybenzoic acid, and then dissolved in vials using diluted ammonia (0.05 M) LC–MS grade (Fluka) to reach a final volume of 1 mL. Samples were injected by an Agilent 1200 G1367 autosampler in two replicates using 40 µl of solution for each analysis. Mass spectra were obtained with an LTQ Orbitrap (Thermo Electron, Waltham, MA) equipped with

Table 1
Mass yields, elemental analysis and percent visibility of organic matter of wheat cropped soil in eSOM and Humeomic fractions, as evaluated by referring to internal standards in GC–MS and ESI-Orbitrap-MS.

SAMPLE	C%	H%	N%	C/N ratio	Mass yield (mg)	C (mg)[a]	H (mg)[a]	N (mg)[a]	OM_{tot} (mg)[b]	OM_{vis} (mg)[c]	Visibility (%)[d]
Soil 1st year	1.05 ± 0.05	n.d.	0.08 ± 0.002	**13.13**	100000	**1050 ± 50**	n.d.	**80 ± 2**	n.d.	n.d.	n.d.
eSOM	17.7 ± 0.1	3.8 ± 0.1	1.9 ± 0.01	**9.33**	**1086 ± 20**	**192.2 ± 3.5**	**41.3 ± 1.1**	**20.6 ± 0.1**	**455.46**	**184.01**	**40.4**
RES[e]	0.49 ± 0.01	n.d.	0.03 ± 0.001	**16.31**	98000 ± 20	482.7 ± 9.8	n.d.	29.6 ± 1.0	n.d.	n.d.	n.d.
Loss of material[f]	41.04	n.d.	3.26	**12.59**	914 ± 20	375.1	n.d.	29.8	n.d.	n.d.	n.d.
ORG1	28.3 ± 0.1	8.1 ± 0.1	0.7 ± 0.01	**44.00**	31 ± 1	8.8 ± 0.3	2.5 ± 0.3	0.2 ± 0.03	11.53	11.53	100
ORG2	34.2 ± 0.2	7.4 ± 0.1	1.1 ± 0.01	**31.30**	302 ± 15	103.3 ± 5.1	22.3 ± 2.6	3.3 ± 0.03	148.24	148.24	100
AQU2	17.4 ± 0.1	4.7 ± 0.1	2.5 ± 0.01	**7.11**	37 ± 2	6.4 ± 0.1	1.7 ± 0.1	0.9 ± 0.04	20.61	2.27	11
ORG3	22.7 ± 0.1	4.5 ± 0.1	0.8 ± 0.01	**26.00**	46 ± 2	10.4 ± 0.2	2.1 ± 0.1	0.4 ± 0.04	13.74	13.74	100
AQU3	9.9 ± 0.1	3.3 ± 0.1	1.4 ± 0.01	**7.00**	7 ± 1	0.7 ± 0.01	0.2 ± 0.01	0.1 ± 0.01	n.d.	n.d.	n.d.
AQU4	1.6 ± 0.05	4.3 ± 0.1	0.2 ± 0.01	**8.00**	12300 ± 80	196.8 ± 6.0	528.9 ± 12.0	24.6 ± 1.2	627.00	469.62	74.9
RESOM	3.5 ± 0.1	2.5 ± 0.1	0.3 ± 0.01	**11.77**	1310 ± 20	45.9 ± 1.3	32.8 ± 1.0	3.9 ± 0.6	**127.91**	**44.51**	**34.8**
ORGs[g]	32.32 ± 1.5	7.10 ± 0.8	1.03 ± 0.3	31.41	379 ± 18	122.5 ± 5.6	26.9 ± 3.0	3.9 ± 1.0	173.51	173.51	100
RESOM &AQUs[h]	1.83 ± 0.05	4.13 ± 0.02	0.22 ± 0.02	8.47	13654 ± 103	249.8 ± 7.5	563.6 ± 3.0	29.5 ± 2.1	775.52	516.40	66.6
Total HUMEOMICS[i]	2.65 ± 0.09	4.21 ± 0.04	0.24 ± 0.02	**11.15**	**14033 ± 121**	**372.3 ± 13.1**	**590.5 ± 6.0**	**33.4 ± 3.1**	**949.03**	**689.91**	**72.7**
RES[j]	0.74 ± 0.01	n.d.	0.07 ± 0.01	**10.60**	65500 ± 125	484.7 ± 4.9	n.d.	45.9 ± 4.9	n.d.	n.d.	n.d.
Loss of material[k]	0.94	n.d.	0.003	**275.71**	20467 ± 125	193.0	n.d.	0.7	n.d.	n.d.	n.d.
Soil 3rd year	1.11 ± 0.02	n.d.	0.08 ± 0.002	**13.88**	100000	**1110.0 ± 30**	n.d.	**80 ± 2**	n.d.	n.d.	n.d.
eSOM	17.0 ± 0.1	2.1 ± 0.1	1.6 ± 0.01	**10.63**	**1019 ± 30**	**173.2 ± 3.0**	**21.4 ± 0.7**	**16.3 ± 0.3**	**399.87**	**167.14**	**41.8**
RES[e]	0.38 ± 0.01	n.d.	0.06 ± 0.002	**6.35**	97800 ± 30	372.6 ± 9.8	n.d.	58.7 ± 2.0	n.d.	n.d.	n.d.
Loss of material[f]	47.86	n.d.	0.42	**113.04**	1181 ± 30	565.2	n.d.	5.0	n.d.	n.d.	n.d.
ORG1	61.8 ± 0.2	6.5 ± 0.1	0.6 ± 0.01	**49.50**	16 ± 1	9.9 ± 0.6	1.0 ± 0.07	0.2 ± 0.01	12.91	10.51	81.4
ORG2	31.1 ± 0.1	0.6 ± 0.1	1.0 ± 0.01	**31.09**	330 ± 10	102.6 ± 3.1	2.0 ± 0.06	3.3 ± 0.1	152.44	43.60	28.6
AQU2	36.6 ± 0.2	3.1 ± 0.1	4.3 ± 0.01	**8.36**	32 ± 2	11.7 ± 0.7	1.0 ± 0.06	1.4 ± 0.09	21.55	5.62	26.1
ORG3	6.7 ± 0.2	1.1 ± 0.1	1.4 ± 0.01	**12.33**	110 ± 8	7.4 ± 0.5	1.2 ± 0.09	0.6 ± 0.11	9.89	1.69	17.1
AQU3	3.8 ± 0.1	2.0 ± 0.1	0.2 ± 0.01	**4.75**	50 ± 2	1.9 ± 0.1	1.0 ± 0.04	0.4 ± 0.01	n.d.	n.d.	n.d.
AQU4	1.6 ± 0.1	0.2 ± 0.1	0.7 ± 0.01	**16.17**	2326 ± 50	37.2 ± 0.8	4.7 ± 0.1	2.3 ± 0.35	106.69	106.69	100
RESOM	3.8 ± 0.1	0.2 ± 0.1	0.5 ± 0.01	**12.55**	660 ± 25	25.1 ± 1.0	1.0 ± 0.05	2.0 ± 0.13	**55.07**	**16.91**	**30.7**
ORGs[g]	26.29 ± 1.1	0.92 ± 0.1	0.90 ± 0.1	29.24	456 ± 19	119.9 ± 4.2	4.2 ± 0.22	4.1 ± 0.22	175.24	55.80	31.8
RESOM & AQUs[h]	2.47 ± 0.06	0.25 ± 0.01	0.20 ± 0.01	12.44	3068 ± 79	75.9 ± 2.6	7.7 ± 0.25	6.1 ± 0.58	183.31	129.22	70.5
Total HUMEOMICS[i]	5.6 ± 0.1	0.3 ± 0.05	0.3 ± 0.05	**19.20**	**3524 ± 98**	**195.8 ± 6.8**	**11.9 ± 0.47**	**10.2 ± 0.8**	**358.55**	**185.02**	**51.6**
RES[j]	0.36 ± 0.005	n.d.	0.04 ± 0.002	**8.99**	85400 ± 100	307.4 ± 0.4	n.d.	34.2 ± 0.04	n.d.	n.d.	n.d.
Loss of material[k]	5.48	n.d.	2.91	**17.04**	11076 ± 100	606.8	n.d.	35.6	n.d.	n.d.	n.d.

[a] CHN mass yields (mg) calculated by elemental analysis percentages multiplied by the mass yields (mg) of original materials and extracts. For soil, RES and loss of material H was not calculated by elemental analysis and therefore mass yields were not defined (n.d.).
[b] Chromatographic OM_{tot} calculation is explained in Materials and Methods section 2.5.
[c] Chromatographic OM_{vis} calculation is based on internal standard.
[d] Visibility (%) is based on the percentage of Chromatographic OM_{vis} to the relative Chromatographic OM_{tot}.
[e] RES corresponds to residual material after eSOM extraction.
[f] Loss of material after eSOM extraction based on original soil excluding eSOM CHN yields.
[g] ORGs refer to the overall of ORG1, ORG2 and ORG3.
[h] RESOM& AQUs refer to the overall of AQU2, AQU3, AQU4 and RESOM.
[i] Total Humeomics refers to the addition of ORG1, ORG2, AQU2, ORG3, AQU3, AQU4 and RESOM fractions. Humeomics and eSOM extractions were conducted in triplicates. The values are referring to the average.
[j] RES corresponds to residual material at the end of Humeomics after RESOM extraction.
[k] Loss of material at the end of Humeomics after RESOM extraction based on original soil excluding Total Humeomics CHN yields.

a HESI-II source, using negative mode, 140–2000 m/z mass scan range, and 1.0 s scan time. N_2 was the sheath gas (50 AU) and He was the collision gas (5 AU). Ion spray, capillary and tube lens voltages were set to 4000, 200 and 75 V, respectively. The ion source vaporizer and capillary temperatures were set to 350 and 275 °C, respectively. HPSEC comprised an Agilent 1200 G1312 Binary Pump set to output 0.5 mL min^{-1} of a 55/45 A/B solution (A: 5 mM $AcONH_4$ in Milli-Q water and 5% MeCN, pH 7; B: 100% MeCN) for a total of 70 min in a Phenomenex Bio-Sep SEC-S 2000 column (300 × 7.8 mm) and precolumn (30 × 7.8 mm), both thermostatted at 30 °C by an Agilent 1200 G1316 unit. UV chromatogram recordings were ensured by an Agilent 1200 G1315 DAD spectrophotometer set at 254 nm wavelength. The averaged m/z values measured by Orbitrap MS were extracted from the Xcalibur software with $C_{0\text{-}60}$ $H_{0\text{-}120}$ $O_{0\text{-}30}$ $N_{0\text{-}10}$ $Fe_{0\text{-}3}$ limits and 5 ppm mass tolerance, corrected on the basis of the internal standards, and converted to nominal masses by adding the mass of H^+ and removing the masses of FeO, Fe_2O_2, or Fe_3O_3, when necessary. The most probable chemical structure for each empirical formula was found by the ChemSpider (http://www.chemspider.com), and the PubChem (https://pubchem.ncbi.nlm.nih.gov/) databases. As for GC–MS, the signals selected for identification were those exceeding the cut-off limit of 0.05% of the overall area. Identified peaks were then recalculated to match an overall relative percentage of 100.

2.4.3. Elemental analysis

Elemental Composition (C, H, N) of powdered samples (Table 1) was determined with a Fisons Instruments EA 1108 Elemental Analyzer, using Eager 200 Ver. 3.09 calculation software.

2.4.4. Atomic adsorption spectrophotometry

A sample (2 g) of the soil prior to the extractions was suspended overnight in 2 mL of HCl (37%) and then added to 48 mL of Milli-Q water. The suspension was filtered through Whatman 41 filters and Fe in the filtered solution was measured by a Perkin Elmer AA700 Atomic Adsorption Spectrometer (AAS) in the graphite furnace mode. For both 1st and 3rd year wheat cropped soil the Fe content was found to be 2.37 ± 0.05%.

2.5. Calculation of empirical formula

A specific empirical formula $C_xH_yO_zN_aFe_b$ obtained from MS spectra, can be turned into its Formula Molecular Weight (*FMW*), $FMW = 12x + 1y + 16z + 14a + 56b$, where the atomic weight of each element is multiplied by the number of corresponding atoms in each compound. In the case of carbon atoms, the percent of total carbon (C_{tot}) for all the identified compounds in each fraction is obtained by the following equation:

$$\sum_{i=1}^{n} \frac{12x_i \times (abundance_i\%)}{100} = C_{tot}$$

where ($12x_i$) and ($abundance_i\%$) are the total atomic weight and the relative percentage of each i^{th} molecule over the all visible compounds in the mass spectrogram for every fraction.

The total OM (OM_{tot}) for all the identified compounds in each fraction can be similarly calculated by taking into account the *FMW* of each fraction (FMW_i):

$$\sum_{i=1}^{n} \frac{FMW_i \times (abundance_i\%)}{100} = OM_{tot}$$

Then, the percent of OM identified in each Humeomic fraction ($\%\,OM$) can be calculated as follows:

$$\frac{OM_{tot} \times C_i}{C_{tot}} = \%\,OM$$

Where C_i is the percent carbon found in that fraction by elemental analysis. The actual *OM* weight (mg) in each fraction (m_{OMi}) can then be obtained:

$$\frac{(\%\,OM) \times m_i}{100} = m_{OMi}$$

The OM chromatographic visibility of each fraction ($m_{OMi,vis}$) for both ESI-Orbitrap and GC measurements is calculated by multiplying m_{OMi} with the percent visibility reported in Table 1:

$$m_{OMi} \times \%\,visibility = m_{OMi,vis}$$

Finally, the total chromatographic OM can be calculated:

$$\sum_{i=1}^{n} m_{OMi} = m_{OM1} + m_{OM2} + \ldots + m_{OMn}$$

as well as the total visible chromatographic OM:

$$\sum_{i=1}^{n} m_{OMi,vis} = m_{OM1,vis} + m_{OM2,vis} + \ldots + m_{OMn,vis}$$

3. Results and discussion

3.1. Tillage effect on SOM dynamics of a wheat-cropped soil

The molecules composing eSOM and the other Humeomic fractions (Table S1) were identified by ESI-Orbitrap-MS and GC–MS, while their analytical visibility was calculated, based on mass yields and elemental composition (Table 1).

While only 30 mg OC per 100 g of soil were lost from the maize cropped soil after 3 years of tillage (Drosos and Piccolo, 2018), the total soil OC under wheat was slightly, though insignificantly, enhanced by 60 mg per 100 g of soil at the 3rd tillage year, as revealed by elemental analysis (Table 1). Such addition of 3% OC per year due to wheat, is similar to the 3% of SOC turnover per year in a surface soil under *Triticum aestivum* earlier reported by Leavitt et al. (2001). Conversely, the eSOM extract from the 3rd year soil was 19 mg OC smaller than for the 1st year. Even larger was the OC reduction (47.4%) shown by the sum of Humeomics fractions at the 3rd tillage year under wheat cultivation, being the AQU4 and RESOM fractions most responsible for this loss (Table 1). This substantial OC decrease, estimated by elemental analysis for the total Humeomics fractions, indicates that wheat cropping failed to stabilize small-sized labile molecules, probably added to soil by root exudation, which were then lost during the separation procedures.

3.1.1. Single step alkaline extraction of SOM (eSOM)

The molecular composition of eSOM at the 1st year showed that the most abundant compounds belonged to the heterocyclic nitrogen (HN) class, followed by aliphatic ethers (ET), phenolic esters and/or ethers (PE), and heterocyclic oxygen (HO). HN remained the main group in the 3rd year, whereas ET, PE and HO were either degraded or lost, and amides (AD), amines (AM), dicarboxylic (DA), fatty (FA), and hydroxy (HA) acids were extracted in larger yields than in the 1st year (Fig. 1). Concomitantly, the molecules found common in eSOM in both years showed a lesser abundance in the 3rd year (Fig. 2). These results suggest that wheat cropping should have induced a partial destabilization of SOM hydrophobic components with tillage, thereby releasing polar compounds from their hydrophobic segregation (Spaccini et al., 2002) and enabling their solubilization in the alkaline extraction medium.

3.1.2. Humeomics fractionation of SOM

After the first tillage year, HN was confirmed, similarly to eSOM, as the main component in the total Humeomics fractions, along with FA, DA, HA, AM, although benzoic (BA) and phenolic (PA) acids, phenols (PH), and sugars (SU) were additionally identified as significant classes of compounds. However, these compounds were either less abundant or depleted in the soil Humeome at the 3rd tillage year, with the exception

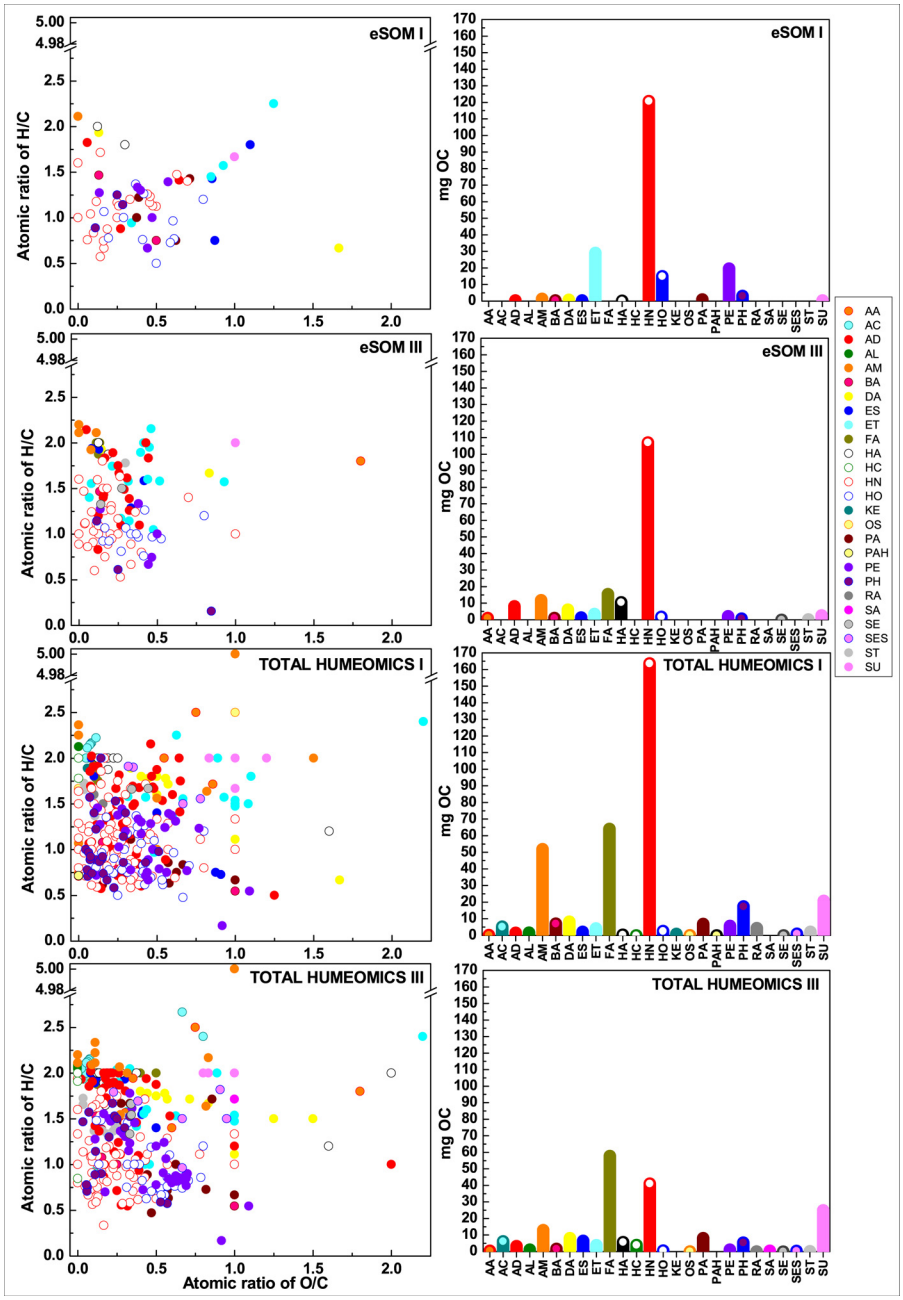

Fig. 1. Weight distribution (mg OC) and Van Krevelen Plots for compounds detected in eSOM, and Total Humeomics after 1st (I) and 3rd (III) year wheat cultivation. AA: Aminoacids, AC: Alcohols, AD: Amides, AL: Alkanes/Alkenes/Alkynes, AM: Amines, BA: Benzoic Acids, DA: Dicarboxylic Acids, ES: Aliphatic Esters, ET: Ethers, FA: Fatty Acids, HA: Hydroxy Acids, HC: Hydrocarbons not assigned elsewhere, HN: Heterocyclic Nitrogen compounds, HO: Heterocyclic Oxygen compounds, KE: Ketones, OS: Organic Sulfur compounds, PA: Phenolic Acids, PAH: Polycyclic Aromatic Hydrocarbons, PE: Phenolic Esters, PH: Phenols, RA: Resin Acids, SA: Sugar Acids, SE: Steroids, SES: Sugar Esters, ST: Sterols, SU: Sugars. Standard deviation for all classes of compounds was ≤ 0.5 mg.

of FA and SU (Fig. 1). The more accurate molecular information obtained by Humeomics in respect to the traditional eSOM extract, indicate that while SOM lost labile components under wheat cropping, the increased concentration of organosoluble/hydrophobic compounds in soil was large enough to protect SOC from further degradation/loss, and preserve, if not increase, the total OC in soil (Table 1).

The molecules identified in the unbound ORG1 fraction as common in both the 1st (I) and 3rd (III) year (Fig. 2), may have been transferred with time from ORG2 and ORG3 fractions (Table S1). However, the more oxidized (I) molecules and alcohols (AC) (Fig. S1) were substituted in ORG 1 by FA (III) of larger molecular size (Fig. S2 and Table 2). Similar trends were noted for the strongly ester-bound organosoluble fraction (ORG3) (Fig. 2), which lost PH (I) (Table 2) in favor of FA (III) (Figs. S1 and S2). Nevertheless, the molecules found common for both tillage years in ORG3 (and to a lesser extend in RESOM) raised in both percentage and concentration in the third year (Fig. 2 and Table S1), thus suggesting that some apolar esterified molecules in the Humeome had been strongly bound to the soil matrix. The opposite trend was detected for the weakly ester-bound hydrosoluble (AQU2) and organosoluble (ORG2) fractions, for which the molecules common to both years decreased with tillage time (Fig. 2). However, the OM turnover in AQU2 favored less oxidized AM and FA over HN compounds (Fig. S3 and Table 2), while in ORG2 the new (III) molecules were placed in the more oxidized region of the van Krevelen plot (Fig. 2).

The AQU4 fraction contained molecules mainly bound to iron hydroxides (Table S1). We showed earlier (Drosos and Piccolo, 2018) that iron complexation to humic molecules is a major mechanism of SOM stabilization. Here, the AQU4 of this study revealed the smallest degree of molecular turnover with time (Fig. 2), comprising only few substitutions of AM molecules with HN compounds (Fig. S3 and S4). This behavior suggests again that the Humeome stability in AQU4 is attributable to complexes with iron (Fig. 3). However, the covalent bonds of Fe (C-O-Fe and C-N(H)-Fe) with humic molecules (Fig. S4), identified

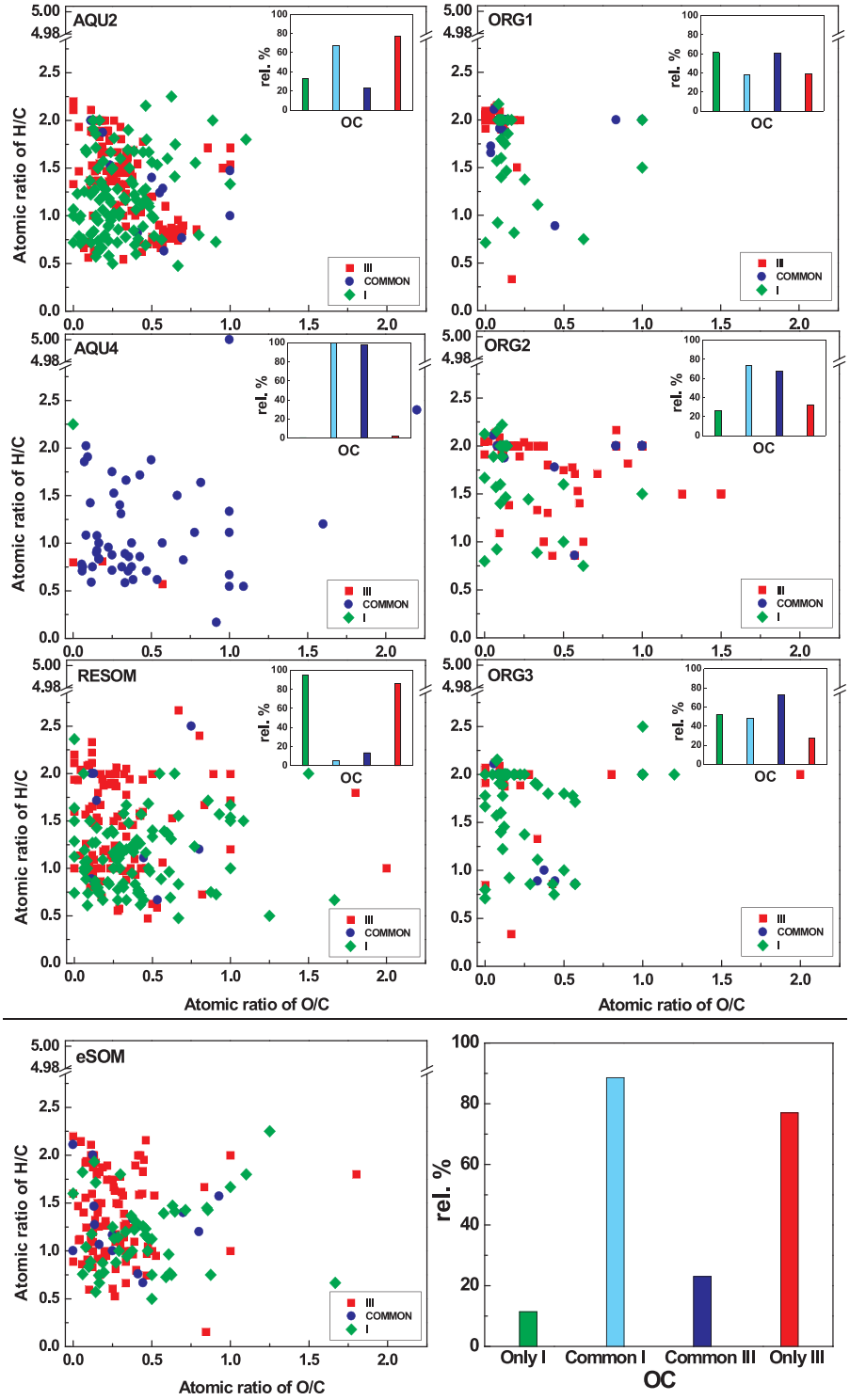

Fig. 2. Van Krevelen Plots of eSOM and Humeomic fractions molecules and their relative OC percentages. Molecules present in both 1st and 3rd year samples are noted in blue dots, their relative OC percentage in the 1st year is set as light blue bar (Common I) and as dark blue bar for the 3rd year (Common III). Molecules present only in the first year are shown in green dots and their relative OC percentage as green bar (Only I), while molecules present only in the third year are shown in red, and their relative OC percentage as red bar (Only III).

by Orbitrap MS, were not in the oxidized Fe^{3+}, but in the reduced Fe^{2+} state, and in non-crystalline but amorphous structures (XRD data not shown). This should be due to the reducing properties of the soil Humeome (Aeschbacher et al., 2012), since humic matter is well known to act as electron donor and capable to effectively reduce the native soil Fe^{3+} oxides *in situ* (Peretyazhko and Sposito, 2006). However, in the case of wheat, the molecules bound to iron in AQU4 (III) were less than in AQU4 (I), thereby suggesting that such larger loss of AQU4 (III) material during dialysis than for maize (Drosos and Piccolo, 2018), may have been probably due to the observed greater hydrophylicity of SOM under wheat.

In RESOM, the maximum structural turnover found in the 3rd year, was attributed to the reduction of the molecular size (Fig. S4) of lipid molecules (Fig. 2), such as FA, DA, and AC, to the increase of reduced

Table 2
Compounds classes mg OC and (%) in eSOM and Humeomic fractions from soils after 1st and 3rd year of wheat cultivation.

	1st year (I)									
Sample										
Group	eSOM	ORG1	ORG2	ORG3	AQU2	AQU4	RESOM	Total ORGs	Total AQUs &RESOM	Humeomics Total[a]
AA	–	–	–	–	–	–	0.18(0.4)	**–**	**0.18(0.07)**	**0.18(0.05)**
AC	–	3.67(41.7)	1.45(1.4)	0.08(0.8)	–	–	0.05(0.1)	**5.20(4.23)**	**0.05(0.02)**	**5.25(1.41)**
AD	**0.38(0.2)**	–	–	–	0.05(0.7)	0.98(0.5)	0.50(1.1)	–	**1.53(0.62)**	**1.53(0.41)**
AL	–	–	1.65(1.6)	–	–	–	–	**1.65(1.34)**	–	**1.65(0.44)**
AM	**1.35(0.7)**	–	–	–	0.01(0.2)	51.56(26.2)	0.28(0.6)	–	**51.85(20.85)**	**51.85(13.95)**
BA	**0.38(0.2)**	–	–	–	–	7.08(3.6)	traces(nn)	–	**7.08(2.85)**	**7.08(1.91)**
DA	**0.77(0.4)**	0.03(0.4)	8.06(7.8)	0.07(0.7)	–	traces(nn)	0.09(0.2)	**8.14(6.62)**	**0.09(0.04)**	**8.25(2.22)**
ES	**0.38(0.2)**	0.11(1.2)	1.65(1.6)	0.05(0.5)	0.06(1.0)	–	0.23(0.5)	**1.87(1.52)**	**0.23(0.09)**	**2.10(0.57)**
ET	**29.03(15.1)**	–	–	–	0.38(5.9)	0.59(0.3)	3.21(7.0)	–	**4.18(1.68)**	**4.18(1.12)**
FA unsat.	–	1.05(11.9)	6.40(6.2)	0.53(5.1)	0.01(0.15)	–	0.23(0.5)	**7.98(6.5)**	**0.24(0.1)**	**8.22(2.21)**
FA sat.	–	2.70(30.7)	48.45(46.9)	4.60(44.0)	0.03(0.45)	–	0.05(0.1)	**55.75(45.37)**	**0.08(0.03)**	**55.83(15.02)**
FA total	–	3.75(42.6)	54.85(53.1)	5.13(49.1)	0.04(0.6)	–	0.28(0.6)	**63.73(51.87)**	**0.32(0.13)**	**64.05(17.23)**
HA	**0.19(0.1)**	–	–	0.16(1.5)	0.03(0.4)	0.20(0.1)	–	**0.16(0.13)**	**0.23(0.09)**	**0.39(0.11)**
HC	–	–	–	0.03(0.3)	–	–	–	**0.03(0.02)**	–	**0.03(0.01)**
HN	**120.72(62.8)**	0.03(0.4)	1.55(1.5)	0.24(2.3)	5.21(81.1)	118.48(60.2)	38.09(83.1)	**1.82(1.48)**	**161.78(65.04)**	**163.6(44.02)**
HO	**14.99(7.8)**	–	–	–	0.07(1.1)	1.18(0.6)	1.33(2.9)	–	**2.58(1.04)**	**2.58(0.69)**
KE	–	–	0.83(0.8)	–	–	–	–	**0.83(0.68)**	–	**0.83(0.22)**
OS	–	–	–	0.06(0.6)	–	–	–	**0.06(0.05)**	–	**0.06(0.02)**
PA	**0.96(0.5)**	0.11(1.2)	5.68(5.5)	0.89(8.5)	0.02(0.3)	traces(nn)	0.14(0.3)	**6.68(5.44)**	**0.16(0.06)**	**6.84(1.84)**
PAH	–	0.03(0.4)	–	–	–	–	–	**0.03(0.02)**	–	**0.03(0.01)**
PE	**19.61(10.2)**	0.04(0.5)	0.52(0.5)	0.17(1.6)	0.03(0.4)	4.33(2.2)	0.60(1.3)	**1.03(0.84)**	**4.66(1.87)**	**5.69(1.53)**
PH	**3.08(1.6)**	0.08(0.9)	1.76(1.7)	2.9(27.8)	0.06(0.9)	12.0(6.1)	0.55(1.2)	**4.74(3.86)**	**12.61(5.07)**	**17.35(4.67)**
RA	–	0.39(4.4)	3.5(3.4)	0.45(4.3)	traces(nn)	–	–	**4.34(3.53)**	**traces(nn)**	**4.34(1.17)**
SA	–	–	–	–	–	–	–	–	–	–
SE	–	–	–	–	traces(nn)	traces(nn)	–	–	**traces(nn)**	**traces(nn)**
SES	–	–	–	0.05(0.5)	0.47(7.3)	0.4(0.2)	–	**0.05(0.04)**	**0.87(0.35)**	**0.92(0.25)**
ST	–	0.34(3.8)	1.76(1.7)	–	0.01(0.1)	–	–	**2.10(1.71)**	**0.01(nn)**	**2.11(0.57)**
SU	**0.38(0.2)**	0.22(2.5)	20.04(19.4)	0.16(1.5)	–	–	0.32(0.7)	**20.42(16.62)**	**0.32(0.13)**	**20.74(5.58)**
					3rd year (III)					
AA	**1.04(0.6)**	–	0.31(0.3)	–	–	–	0.13(0.5)	**0.31(0.26)**	**0.13(0.18)**	**0.44(0.23)**
AC	–	1.14(11.5)	2.26(2.2)	0.21(2.9)	0.02(0.2)	–	2.51(10.0)	**3.61(3.01)**	**2.53(3.42)**	**6.14(3.17)**
AD	**8.14(4.7)**	–	0.31(0.3)	–	0.52(4.4)	1.3(3.5)	1.15(4.6)	**0.31(0.26)**	**2.97(4.01)**	**3.28(1.69)**
AL	–	0.33(3.3)	0.72(0.7)	0.07(0.1)	–	–	–	**1.12(0.94)**	–	**1.12(0.58)**
AM	**11.78(6.8)**	–	0.92(0.9)	–	3.86(32.9)	1.12(3.0)	7.02(28.0)	**0.92(0.77)**	**12(16.21)**	**12.92(6.66)**
BA	**1.04(0.6)**	–	0.72(0.7)	–	0.39(3.3)	0.07(0.2)	0.5(2.0)	**0.72(0.6)**	**0.96(1.3)**	**1.68(0.87)**
DA	**6.06(3.5)**	–	5.43(5.3)	0.04(0.6)	0.3(2.6)	0.07(0.2)	2.23(8.9)	**5.47(4.56)**	**2.6(3.51)**	**8.07(4.16)**
ES	**1.39(0.8)**	0.10(1.0)	5.43(5.3)	0.6(8.1)	0.32(2.7)	–	0.03(0.1)	**6.13(5.11)**	**0.35(0.47)**	**6.48(3.34)**
ET	**3.46(2.0)**	–	3.49(3.4)	–	0.09(0.8)	0.04(0.1)	0.2(0.8)	**3.49(2.91)**	**0.33(0.45)**	**3.82(1.97)**
FA unsat.	**5.72(3.3)**	1.28(12.9)	0.83(0.8)	0.05(0.7)	0.25(2.1)	–	0.67(2.7)	**2.16(1.8)**	**0.92(1.24)**	**3.08(1.59)**
FA sat.	**9.70(5.6)**	5.80(58.6)	39.70(38.7)	4.56(61.7)	1.94(16.6)	–	2.64(10.5)	**50.06(41.76)**	**4.58(6.19)**	**54.64(28.18)**
FA total	**15.42(8.9)**	7.08(71.5)	40.53(39.5)	4.61(62.4)	2.19(18.7)	–	3.31(13.2)	**52.22(43.56)**	**5.50(7.43)**	**57.72(29.77)**
HA	**10.57(6.1)**	0.64(6.5)	4.21(4.1)	0.12(1.6)	0.29(2.5)	traces(nn)	0.48(1.9)	**4.97(4.15)**	**0.77(1.04)**	**5.74(2.96)**
HC	–	0.15(1.5)	3.38(3.3)	0.44(6.0)	–	–	–	**3.97(3.31)**	–	**3.97(2.05)**
HN	**107.06(61.8)**	0.03(0.3)	3.38(3.3)	0.38(5.1)	2.6(22.2)	30.01(80.6)	4.63(18.5)	**3.79(3.16)**	**37.24(50.32)**	**41.03(21.16)**
HO	**1.73(1.0)**	–	–	–	0.20(1.7)	0.07(0.2)	0.33(1.3)	–	**0.6(0.81)**	**0.60(0.31)**
KE	–	–	–	–	–	–	–	–	–	–
OS	–	0.10(1.0)	–	–	–	–	–	**0.1(0.08)**	–	**0.10(0.05)**
PA	–	0.05(0.5)	6.99(6.8)	0.72(9.8)	0.23(2.0)	0.04(0.1)	0.05(0.2)	**7.76(6.47)**	**0.32(0.43)**	**8.08(4.17)**
PAH	–	–	–	–	–	–	–	–	–	–
PE	**2.08(1.2)**	0.03(0.4)	–	–	0.25(2.1)	0.22(0.6)	0.65(2.6)	**0.03(0.03)**	**1.12(1.51)**	**1.15(0.59)**
PH	**0.69(0.4)**	–	–	–	0.15(1.3)	4.21(11.3)	1.05(4.2)	–	**5.41(7.31)**	**5.41(2.79)**
RA	–	–	–	–	–	–	0.13(0.5)	–	**0.13(0.18)**	**0.13(0.07)**
SA	–	–	–	–	0.2(1.7)	–	0.28(1.1)	–	**0.48(0.65)**	**0.48(0.25)**
SE	**traces(nn)**	–	–	–	traces(nn)	traces(nn)	–	–	**traces(nn)**	**traces(nn)**
SES	–	–	0.31(0.3)	–	0.01(0.1)	0.07(0.2)	–	**0.31(0.26)**	**0.08(0.11)**	**0.39(0.2)**
ST	**0.17(0.1)**	0.15(1.5)	–	–	0.09(0.8)	–	–	**0.15(0.13)**	**0.09(0.12)**	**0.24(0.12)**
SU	**2.6(1.5)**	0.1(1.0)	24.21(23.6)	0.18(2.5)	–	–	0.4(1.6)	**24.49(20.43)**	**0.4(0.54)**	**24.89(12.84)**

FA total are referring to the sum of the unsaturated (FA unsat.) and saturated (FA sat.) fatty acids.

AD compounds, and to the great losses of HN molecules (Fig. S3). However, the presence of the same molecules in both eSOM and RESOM (Table S1), suggests that some highly hydrophobic humic molecules could be released from the soil matrix only after an aqueous alkaline extraction. This implies that the 24 common molecules, mainly HN, had not undergone any structural transformation during Humeomics, thus indicating that the sequential fractionation did not introduce extraction artifacts. Moreover, since these common molecules decreased from 154.4 mg OC in eSOM (I) to 16.7 mg OC in RESOM (I) after Humeomics, it signifies that they were the components mainly lost during dialysis of the 1st year RESOM (Table 1). By excluding the OC of these molecules from the Humeomics losses, the unknown OC lost in the 1st year was then adjusted to 55.4 mg, thus accounting only for 5.3% of the total OC. However, the 3rd year losses of SOC after Humeomics rose to 54.7%, and remained as large as 48.3% even after exclusion of the OC for the common molecules lost from RESOM (III). This observation reveals

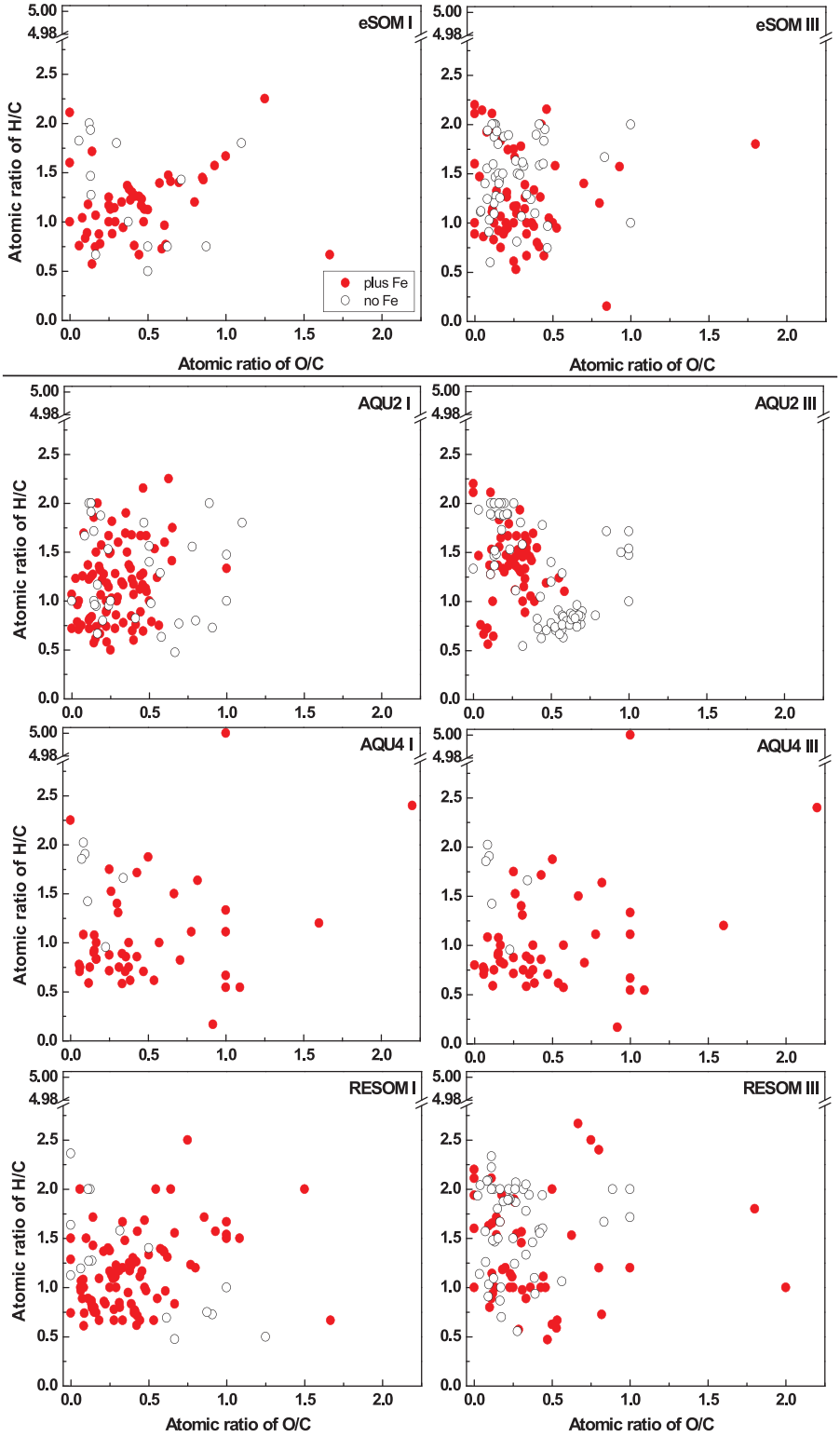

Fig. 3. Van Krevelen plots of molecular structures in eSOM, AQU and RESOM fractions for both wheat cropped years. Molecules linked to iron hydroxides are shown in red. AQU4 being the fraction with the highest mass of iron is more stable among the 1st and 3rd year. For AQU2, RESOM fractions and eSOM there are abundant molecules in the 3rd year non bound to iron.

once more that the effect of tillage transformed SOM to less hydrophobic and more labile structures, and that wheat cultivation magnifies this process more than maize (Drosos and Piccolo, 2018).

3.2. Effects of wheat versus maize cropping on SOM dynamics

It has been earlier shown that traditional tillage affected the Humeome of a soil cropped with maize over a 3 years period (Drosos and Piccolo, 2018). Here, we applied Humeomics to the same soil and tillage system but under wheat cropping, in order to show the

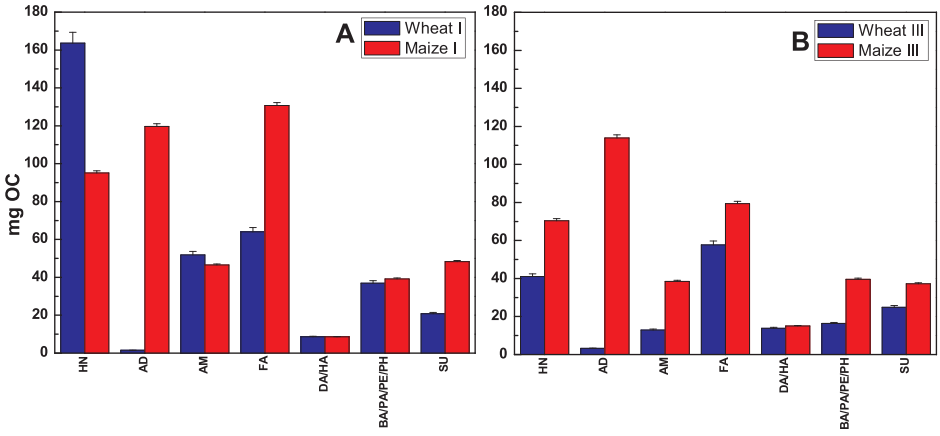

Fig. 4. Differences of the SOM main groups (mg OC) extracted by Humeomics in total and identified by ESI-Orbitrap-MS (AQU2, AQU4, and RESOM) and GC–MS (ORG1, ORG2, and ORG3), for both Wheat and Maize crops after: A. one year (I), and, B. three years (III) of cultivation. There are 7 main classes of compounds: Heterocyclic nitrogen compounds (HN), amides (AD), amines (AM), fatty acids (FA), other lipidic dicarboxylic (DA) and hydroxy (HA) acids, aromatic compounds such as benzoic (BA) and phenolic (PA) acids, phenolic esters (PE) and phenols (PH), and sugars (SU).

differences on SOM dynamics due to the selected crop. After the 1st tillage year, the labile ORG1 fraction under wheat (Table 1, Table 2, Table S1 and Fig. S1) showed a larger AL oxidation to AC than that found in ORG1 under maize (Drosos and Piccolo, 2018), while ORG2 lost 50% of abundance under wheat (Table 1) as compared to ORG2 under maize (Drosos and Piccolo, 2018), and ORG3 showed a larger reduction of HA to FA, and of PA to PH under wheat (Table 1–2, Table S1 and Fig. S1) than under maize (Drosos and Piccolo, 2018).

In both wheat and maize cropping systems, the Humeome was composed by seven most abundant molecular classes (Fig. 4): three of them represented nitrogen-containing compounds (HN, AD, AM), two were alkyl acids either as linear (FA) or functionalized (DA/HA) carboxylic acids, mainly present into organosoluble fractions, and the other two classes comprised hydrophobic aromatic molecules (BA/PA/PE/PH), and a group of carbohydrate compounds (SU).

While molecular transformation of these classes of compounds due to tillage occurred in both cropping systems, there were specific changes directly linked to the cultivated crop (Fig. 4). The greatest difference was related to AD molecules, that were almost absent in the case of wheat, whereas they represented not only the most abundant group under maize, but also the most stable one (Drosos and Piccolo, 2018). In fact, AD molecules were already reported to be larger in soils cropped over a period of 6 years with maize than with wheat (Chen et al., 2017). While FA were largely abundant under maize after the first tillage year, but were greatly reduced after three years of tillage (Drosos and Piccolo, 2018), their amount remained stable over three years under wheat cropping (Fig. 4). Similarly, soils cropped with wheat for four years were earlier found rich in alkyl compounds, such as FA and AL (Wiesenberg et al., 2010).

In our study, the FA molecules under wheat were progressively degraded, while new plant-derived FA got replenished (Table 2 and Table S1). In fact, the $C_{16:1}$ to $C_{16:0}$ ratio raised from 0.014 to 0.048 (Table 2) from 1st to 3rd year of cropping, thus revealing an increased contribution of microbial derived organic matter. However, since the ratio remained lower than 0.1 in both years, most FA must have originated from plants (Wiesenberg et al., 2010). In fact, the Humeome results for wheat cropping showed that the ratio of unsaturated to saturated FA (Table 2) dropped gradually from the labile ORG1 fraction (0.389 and 0.221 in ORG1 (I) and ORG1 (III), respectively) to the strongly ester-bound ORG3 fraction (0.115 and 0.011 in ORG3 (I) and ORG3 (III), respectively), thus revealing a progressive enhancement of less labile, strongly bound molecules. This may be explained not only with an increase of the hydrophobic protection from microbial degradation, but also with the less favorable conditions to microbial activity in PA and PH rich environments (Fig. S1).

The slight increase of the microbial derived organic material from the first to the third year is also shown by the ratio of the OC mg of microbially-derived SU, such as mannose, galactose, rhamnose and fucose, to the OC mg of plant-derived SU, such as glucose, xylose and arabinose (Table S1) (Larré-Larrouy et al., 2004; Basler et al., 2015; Lu et al., 2016), that changed from 0.76 (1st year wheat) to 0.81 (3rd year wheat). However, such a minor variation was not reflected by the invariance in actinomycetes and total aerobic and anaerobic cellulolytic bacterial populations observed in this soil with tillage (Ventorino et al., 2012), although fungi were found significantly reduced in the 3rd tillage year for both wheat and maize crops. The only significant difference between the two crops was in the 3rd year of cultivation, for which more invertase activity was present under wheat than under maize (Ventorino et al., 2012). Larger levels of invertase may occur due to hydrolysis of sucrose to the more bioavailable glucose and fructose forms, probably related to the smaller content of sugar in SOM under wheat than under maize (Fig. 4).

These findings are in line with previous observations, which reported that wheat straw decomposition enriched SOM with alkyl C (Chen et al., 2018). However, alkyl organic acids with more than one functional groups (DA/HA) were found to be more abundant in the third than in the first year soil, regardless of the cropping system (Fig. 4). While AM and, mainly, HN molecules were more largely represented in the first tillage year for wheat than for maize, they were lost after the third year more under wheat than under maize (Fig. 4). The same trend was observed for all abundant molecules in the Humeome, except for the lipidic FA, DA and HA (Fig. 4), thus confirming previous findings which showed that SOC under wheat cropping became progressively more hydrophilic and labile (Shi et al., 2017).

Since the organic acid fraction of root exudates varies with crops (Hütsch et al., 2002; Wang et al., 2006), it is possible that wheat exudates may hydrolyze SOM more extensively than maize exudates. This process may not only favor the release of labile hydrolyzed humic molecules but also induce further SOM solubilization by displacing humic molecules from complexes with iron (Drosos and Piccolo, 2018; Nuzzo et al., 2018). In fact, it was reported that more root-borne water soluble OC is present in the vicinity of wheat roots (Merbach et al., 1999), and that wheat during the germination exudes 10 times more phytosiderophores than that required for Fe plant uptake, although the siderophores significantly decline after 5 weeks (Oburger et al., 2014). Furthermore, rhizobacteria were found to enhance the phytosiderophores (Richardson et al., 2009) deriving from tryptophan (an amino acid largely abundant in wheat germ), responsible for lateral roots growth (Vacheron et al., 2013).

While it is known that siderophores are related to HN and AD molecules (Balado et al., 2015), we showed earlier that 5-methoxy-tryptophan bound to Fe^{2+} ($C_{12}H_{14}N_2O_3FeO$) was the most abundant molecule of the HN group found in the Humeome of the soil studied here (Drosos et al., 2017; Drosos and Piccolo, 2018). This iron-bound molecular complex was similarly present in SOM after the 1st tillage year under both wheat and maize, and, while it remained constant in

SOM under maize after three years of tillage, it was almost totally depleted from the Humeome under wheat in the 3rd tillage year (Table S1).

This is in line with what earlier reported for the same soil (Spaccini and Piccolo, 2013), where the yield of soil macroaggregates (> 1 mm diameter) was similarly reduced for both the wheat- and maize-cropped soils passing from the 1st to the 3rd tillage year from 12.9% to 10.6%, and from 15.7% to 11.4%, respectively. Conversely, the yields of soil microaggregates (< 0.25 mm) raised from 26.2% to 31.1% under wheat, and decreased from 30.4% to 27.5% under maize. These results indicate a different effect of the two crops on the chemical and/or biological activity towards the cementing capacity of SOM.

4. Conclusions

Our findings suggest that wheat cultivation alters the stabilized conformation of the Humeome in soil by hydrolyzing the esterified matrices and displacing the humic molecules from iron complexes (Nuzzo et al., 2018). These processes were most likely responsible for the observed changes in soil physical structure under the two cropping systems (Spaccini and Piccolo, 2013). Moreover, the great lability of HN and AD molecules, shown by the differences in AD content in either wheat- or maize-cropped soils and in HN between the 1st and 3rd tillage year in soils under wheat cropping (Fig. 4), suggests that the cropping system appears to regulate the molecular composition and dynamics of the soil Humeome. This in line with previous indications that the vegetation type, e.g.: C3 *vs* C4 plants, affects SOM stability, (Luo et al., 2018), and that soil management practices alter the short-term dynamics of the active carbon and nitrogen pools in SOM (Franzluebbers et al., 1994). Evidence for this phenomenon was recently reported by Xiong et al. (2019), who showed that changes in root exudates alter the soil microbiome, thereby resulting in a diverse SOM composition and accumulation in soil. In this work, we confirmed by molecular details that the complex supramolecular arrangements of the soil Humeome was extremely dynamic and related not only to the influence of land management (Piccolo et al., 2018), but also to its cropping system.

Declaration of interests

The authors declare that they have no known competing financial interests or personal relationships that could have appeared to influence the work reported in this paper.

Acknowledgements

The authors are grateful to Prof. Paola Vitaglione for access to ESI-Orbitrap-MS, to Mr. Franco Scognamiglio for assistance in metal analyses and Mrs. Claudia Savarese for assistance in the extractions.

Appendix A. Supplementary data

Supplementary material related to this article can be found, in the online version, at doi:https://doi.org/10.1016/j.still.2019.104448.

References

Aeschbacher, M., Graf, C., Schwarzenbach, R.P., Sander, M., 2012. Antioxidant properties of humic substances. Environ. Sci. Technol. 46, 4916–4925. https://doi.org/10.1021/es300039h.

Balado, M., Souto, A., Vences, A., Careaga, V.P., Valderrama, K., Segade, Y., Rodríguez, J., Osorio, C.A., Jiménez, C., Lemos, M.L., 2015. Two Catehol Siderophores, Acinetobactin and Amonabactin, are simultaneously produced by *Aeromonas salmonicida* subsp. *Salmonicida* sharing part of the biosynthetic pathway. ACS Chem. Biol. 10, 2850–2860. https://doi.org/10.1021/acschembio.5b00624.

Basler, A., Dippold, M., Helfrich, M., Dyckmans, J., 2015. Microbial carbon recycling: an underestimated process controlling soil carbon dynamics – part 2: a C3-C4 vegetation change field labeling experiment. Biogeosciences 12, 6291–6299. https://doi.org/10.5194/bg-12-6291-2015.

Batjes, N.H., 2014. Total carbon and nitrogen in the soils of the world. Eur. J. Soil Sci. 65, 4–21. https://doi.org/10.1111/ejss.12114_2.

Baveye, P.C., Berthelin, J., Tessier, D., Lemaire, G., 2018. The "4 per 1000" initiative: a credibility issue for the soil science community? Geoderma 309, 118–123. https://doi.org/10.1016/j.geoderma.2017.05.005.

Bernard, L., Mougel, C., Maron, P.-A., Nowak, V., Lévêque, J., Henault, C., el Zahar Haichar, F., Berge, O., Marol, C., Balesdent, J., Gibiat, F., Lemanceau, P., Ranjard, L., 2007. Dynamics and identification of soil microbial populations actively assimilating carbon from ^{13}C-labelled wheat residue as estimated by DNA- and RNA-SIP techniques. Environ. Microbiol. 9 (3), 752–764. https://doi.org/10.1111/j.1462-2920.2006.01197.x.

Chen, X., Mao, A., Zhang, Y., Zhang, L., Chang, J., Gao, H., Thompson, M.L., 2017. Carbon and nitrogen forms in soil organic matter influenced by incorporated wheat and corn residues. Soil Sci. Plant Nutr. 63 (4), 377–387. https://doi.org/10.1080/00380768.2017.1359797.

Chen, X., Xu, Y., Gao, H.-J., Mao, J., Chu, W., Thompson, M.L., 2018. Biochemical stabilization of soil organic matter in straw-amended, anaerobic and aerobic soils. Sci. Total Environ. 625, 1065–1073. https://doi.org/10.1016/j.scitotenv.2017.12.293.

Drosos, M., Nebbioso, A., Mazzei, P., Vinci, G., Spaccini, R., Piccolo, A., 2017. A molecular zoom into soil Humeome by a direct sequential chemical fractionation of soil. Sci. Total Environ. 586, 807–816. https://doi.org/10.1016/j.scitotenv.2017.02.059.

Drosos, M., Savy, D., Spiteller, M., Piccolo, A., 2018a. Structural characterization of carbon and nitrogen molecules in the Humeome of two different grassland soils. Chem. Biol. Technol. Agric. 5, 14. https://doi.org/10.1186/s40538-018-0127-y.

Drosos, M., Nebbioso, A., Piccolo, A., 2018b. Humeomics: a key to unravel the humusic pentagram. In Humusica: towards a unified classification of humus systems, humus manual, Zanella, A.; Ascher - Junell, J. (Eds.). Appl. Soil Ecol. 123, 513–516. https://doi.org/10.1016/j.apsoil.2017.07.027.

Drosos, M., Piccolo, A., 2018. The molecular dynamics of soil humus as a function of tillage. Land Deg. Dev. 29, 1792–1805. https://doi.org/10.1002/ldr.2989.

Du, C., Goyne, K.W., Miles, R.J., Zhou, J.A., 2014. 1915-2011 microscale record of soil organic matter under wheat cultivation using FTIR-PAS depth-profiling. Agron. Sustain. Dev. 34, 803–811. https://doi.org/10.1007/s13593-013-0201-6.

Franzluebbers, A.J., Hons, F.M., Zuberer, D.A., 1994. Seasonal changes in soil microbial biomass and mineralizable c and n in wheat management systems. Soil Biol. Biochem. 26 (11), 1469–1475. https://doi.org/10.1016/0038-0717(94)90086-8.

Grignani, C., Alluvione, F., Bertora, C., Zavattaro, L., Fagnano, M., Fiorenino, N., Quaglietta Chiarandà, F., Amao, M., Lupo, F., Bochicchio, R., 2012. Field plots and crop yields under innovative methods of carbon sequestration in soil. In: Piccolo, A. (Ed.), Carbon SequEstration in Agricultural Soils. Springer-Verlag, Berlin, Heidelberg, Germany, pp. 39–60. https://doi.org/10.1007/978-3-642-23385-2.

Hütsch, B.W., Augustin, J., Merbach, W., 2002. Plant rhizodeposition-an important source for carbon turnover in soils. J. Plant Nutr. Soil Sci. 165, 397–407. https://doi.org/10.1002/1522-2624(200208)165:4%3C397::AID-JPLN397%3E3.0.CO;2-C.

Lal, R., 2009. Soils and food sufficiency. A review. Agron. Sustain. Dev. 29, 113–133. https://doi.org/10.1051/agro:2008044.

Larré-Larrouy, M.C., Blanchart, E., Albrecht, A., Feller, C., 2004. Carbon and monosaccharides of a tropical Vertisol under pasture and market-gardening: distribution in secondary organomineral separates. Geoderma 119, 163–178. https://doi.org/10.1016/S0016-7061(03)00259-3.

Leavitt, S.W., Pendall, E., Paul, E.A., Brooks, T., Kimball, B.A., Pinter Jr., P.J., Johnson, H.B., Matthias, A., Wall, G.W., LaMorte, R.L., 2001. Stable-carbon isotopes and soil organic carbon in wheat under CO_2 enrichment. New Phytol. 150, 305–314. https://doi.org/10.1046/j.1469-8137.2001.00113.x.

Lu, C., Cao, Y., He, C., Bao, X., Fang, R., Wang, Y., Chen, X., Shi, Y., Li, Q., 2016. Effects of elevated O_3 and CO_2 on the relative contribution of carbohydrates to soil organic matter in an agricultural soil. Soil Till. Res. 159, 47–55. https://doi.org/10.1016/j.still.2016.02.001.

Luo, W., Wang, X., Sardans, J., Wang, Z., Dijkstra, F.A., Lü, X.-T., Peñuelas, J., Han, X., 2018. Higher capability of C3 than C4 plants to use nitrogen inferred from nitrogen stable isotopes along an aridity gradient. Plant Soil 428, 93–103. https://doi.org/10.1007/s11104-018-3661-2.

Marx, M., Buegger, F., Gattinger, A., Zsolnay, Á., Munch, J.C., 2007. Determination of the fate of ^{13}C labelled maize and wheat exudates in an agricultural soil during a short-term incubation. Eur. J. Soil Sci. 58, 1175–1185. https://doi.org/10.1111/j.1365-2389.2007.00911.x.

Merbach, W., Mirus, E., Knof, G., Remus, R., Ruppel, S., Russow, R., Gransee, A., Schulze, J., 1999. Release of carbon and nitrogen compounds by plant roots and their possible ecological importance. J. Plant Nutr. Soil Sci. 162, 373–383. https://doi.org/10.1002/(SICI)1522-2624(199908)162:4<373::AID-JPLN373>3.0.CO;2-#.

Minasny, B., Malone, B.P., McBratnen, A.B., Angers, D.A., Arrouays, D., Chambers, A., Chaplot, V., Chen, Z.-S., Cheng, K., Das, B.S., Field, D.J., Gimona, A., Hedley, C.B., Hong, S.Y., Mandal, B., Marchant, B.P., Martin, M., McConkey, B.G., Mulder, V.L., O'Rourke, S., Richer-de-Forges, A.C., Odeh, I., Padarian, J., Paustian, K., Pan, G., Poggio, L., Savin, I., Stolbovoy, V., Stockman, U., Sulaeman, Y., Tsui, C.-C., Vågen, T.-G., vanWesemael, B., Winowiecki, L., 2017. Soil carbon 4 per mille. Geoderma 292, 59–86. https://doi.org/10.1016/j.geoderma.2017.01.002.

Nebbioso, A., Piccolo, A., 2011. Basis of a Humeomics science: chemical fractionation and molecular characterization of humic biosuprastructures. Biomacromolecules 12, 1187–1199. https://doi.org/10.1021/bm101488e.

Nuzzo, A., De Martino, A., Di Meo, V., Piccolo, A., 2018. Potential alteration of iron-humate complexes by plant root exudates and microbial siderophores. Chem. Biol. Technol. Agric. 5, 19. https://doi.org/10.1186/s40538-018-0132-1.

Oburger, E., Gruber, B., Schindlegger, Y., Schenkeveld, W.D.C., Hann, S., Kraemer, S.M., Wenzel, W.W., Puschenreiter, M., 2014. Root exudation of phytosiderophores from

soil-grown wheat. New Phytol. 203, 1161–1174. https://doi.org/10.1111/nph.12868.
Peretyazhko, T., Sposito, G., 2006. Reducing capacity of terrestrial humic acids. Geoderma 137, 140–146. https://doi.org/10.1016/j.geoderma.2006.08.004.
Piccolo, A., 2002. The supramolecular structure of humic substances: a novel understanding of humus chemistry and implications in soil science. Adv. Agron. 75, 57–134. https://doi.org/10.1016/S0065-2113(02)75003-7.
Piccolo, A., 2016. In memoriam Prof. F.J. Stevenson and the Question of humic substances in soil. Chem. Biol. Technol. Agric. 3, 23. https://doi.org/10.1186/s40538-016-0076-2.
Piccolo, A., Spaccini, R., Cozzolino, V., Nuzzo, A., Drosos, M., Zavattaro, L., Grignani, C., Puglisi, E., Trevisan, M., 2018. Effective carbon sequestration in Italian agricultural soils by *in situ* polymerization of soil organic matter under biomimetic potocatalysis. Land Degrad. Dev. 29, 485–494. https://doi.org/10.1002/ldr.2877.
Putnam, R.J., 1994. Community Ecology. Chapman and Hall, London.
Richardson, A.E., Barea, J.-M., McNeil, A.M., Prigent-Combaret, C., 2009. Acquisition of phosphorus and nitrogen in the rhizosphere and plant growth promotion by microorganisms. Plant Soil 321, 305–339. https://doi.org/10.1007/s11104-009-9895-2.
Schenck zu Schweinsberg-Mickan, M., Jörgensen, R.G., Müller, T., 2012. Rhizodeposition: its contribution to microbial growth and carbon and nitrogen turnover within the rhizosphere. J. Plant Nutr. Soil Sci. 175, 750–760. https://doi.org/10.1002/jpln.201100300.
Shi, H., Wang, X., Xu, M., Zhang, H., Luo, Y., 2017. Characteristics of soil C:N ratio and $\delta^{13}C$ in wheat-maize cropping system of the North China Plain and influences of the Yellow River. Sci. Rep. 7, 16854. https://doi.org/10.1038/s41598-017-17060-3.
Spaccini, R., Piccolo, A., 2013. Effects of field managements for soil organic matter stabilization on water-stable aggregate distribution and aggregate stability in three agricultural soils. J. Geochem. Explor. 129, 45–51. https://doi.org/10.1016/j.gexplo.2012.10.004.
Spaccini, R., Piccolo, A., Conte, P., Haberauer, G., Gerzabek, M.H., 2002. Increased soil organic carbon sequestration through hydrophobic protection by humic substances. Soil Biol. Biochem. 34, 1839–1851. https://doi.org/10.1016/S0038-0717(02)00197-9.
Vacheron, J., Desbrosses, G., Bouffaud, M.-L., Touraine, B., Moënne-Loccoz, Y., Muller, D., Legendre, L., Wisniewski-Dyé, F., Prigent-Combaret, C., 2013. Plant growth-promoting rhizobacteria and root system functioning. Front. Plant Sci. 4, 356. https://doi.org/10.3389/fpls.2013.00356.
Ventorino, V., De Marco, A., Pepe, O., Virzo de Santo, A., Moschetti, G., 2012. Impact of innovative agricultural practices of carbon sequestration on soil microbial community. In: Piccolo, A. (Ed.), Carbon SequEstration in Agricultural Soils. Springer-Verlag, Berlin, Heidelberg, Germany, pp. 147–178. https://doi.org/10.1007/978-3-642-23385-2.
Wang, P., Bi, S., Wang, S., Ding, Q., 2006. Variation of wheat root exudates under aluminum stress. J. Agric. Food Chem. 54, 10040–10046. https://doi.org/10.1021/jf061249o.
Wiesenberg, G.L.B., Dorodnikov, M., Kuzyakov, Y., 2010. Source determination of lipids in bulk soil and soil density fractions after four years of wheat cropping. Geoderma 156, 267–277. https://doi.org/10.1016/j.geoderma.2010.02.026.
Xiong, L., Liu, X., Vinci, G., Spaccini, R., Drosos, M., Li, L., Piccolo, A., Pan, G., 2019. Molecular changes of soil organic matter induced by root exudates in a rice paddy under CO_2 enrichment and warming of canopy air. Soil Biol. Biochem. 137, 107544. https://doi.org/10.1016/j.soilbio.2019.107544.